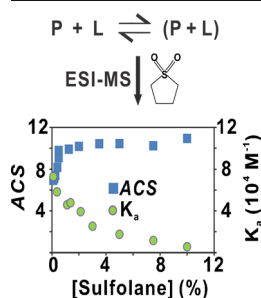RESEARCH ARTICLE

Influence of Sulfolane on ESI-MS Measurements of Protein–Ligand Affinities

Yuyu Yao, Michele R. Richards, Elena N. Kitova, John S. Klassen

Alberta Glycomics Centre and Department of Chemistry, University of Alberta, Edmonton, Alberta T6G 2G2, Canada

Abstract. The results of an investigation into the influence of sulfolane, a commonly used supercharging agent, on electrospray ionization mass spectrometry (ESI-MS) measurements of protein–ligand affinities are described. Binding measurements carried out on four protein–carbohydrate complexes, lysozyme with β-D-GlcNAc-(1→4)-β-D-GlcNAc-(1→4)-β-D-GlcNAc-(1→4)-D-GlcNAc, a single chain variable fragment and α-D-Gal-(1→2)-[α-D-Abe-(1→3)]-α-D-Man-OCH₃, cholera toxin B subunit homopentamer with β-D-Gal-(1→3)-β-D-GalNAc-(1→4)[α-D-Neu5Ac-(2→3)]-β-D-Gal-(1→4)-β-D-Glc, and a fragment of galectin 3 and α-L-Fuc-(1→2)-β-D-Gal-(1→3)-β-D-GlcNAc-(1→3)-β-D-Gal-(1→4)-β-D-Glc, revealed that sulfolane generally reduces the apparent (as measured by ESI-MS) protein–ligand affinities. To establish the origin of this effect, a detailed study was undertaken using the lysozyme–tetrasaccharide interaction as a model system. Measurements carried out using isothermal titration calorimetry (ITC), circular dichroism, and nuclear magnetic resonance spectroscopies reveal that sulfolane reduces the binding affinity in solution but does not cause any significant change in the higher order structure of lysozyme or to the intermolecular interactions. These observations confirm that changes to the structure of lysozyme in bulk solution are not responsible for the supercharging effect induced by sulfolane. Moreover, the agreement between the ESI-MS and ITC-derived affinities indicates that there is no dissociation of the complex during ESI or in the gas phase (i.e., in-source dissociation). This finding suggests that supercharging of lysozyme by sulfolane is not related to protein unfolding during the ESI process. Binding measurements performed using liquid sample desorption ESI-MS revealed that protein supercharging with sulfolane can be achieved without a reduction in affinity.

Keywords: Supercharging, ESI-MS, Protein–ligand affinities, Liquid sample DESI-MS

Introduction

The direct electrospray ionization mass spectrometry (ESI-MS) assay is a valuable tool for detecting and quantifying non-covalent protein–ligand interactions in vitro [1]. In addition to its speed, sensitivity, and selectivity, the assay is free of any requirements of immobilization or labeling of either the protein or the ligand, making it a highly versatile binding assay. Moreover, the method is well suited for screening libraries of compounds to simultaneously identify and quantify the highest affinity ligands [2]. When implemented using a catch-and-release (CaR) format (i.e., CaR-ESI-MS), the assay enables the screening of libraries against high molecular weight (MW) protein assemblies, such as viral capsid protein particles, for which the protein–ligand complexes are difficult to analyze directly by ESI-MS [3]. A semiquantitative ESI-MS assay suitable for screening natural compound libraries at unknown concentrations, such as mixtures of human milk oligosaccharides isolated from breast milk, against target proteins to identify interactions and rank their affinities was also recently described [4].

While these ESI-MS assays allow for the detection and quantification of protein–ligand interactions in vitro, they do not, on their own, provide insight into the location or nature of the interactions. There is evidence that intermolecular interactions are largely preserved upon transfer of protein–ligand complexes from solution to the gas phase using ESI from studies of several protein–ligand complexes using the blackbody infrared radiative dissociation/functional group replacement strategy [5–10]. Consequently, one possible strategy for localizing ligand binding sites involves so-called "top-down"

Correspondence to: John S. Klassen; *e-mail:* john.klassen@ualberta.ca

MS using electron-mediated activation methods, such as electron capture dissociation (ECD) and electron transfer dissociation (ETD). With this approach, the identification of peptide fragments retaining the ligand serves to localize the binding site(s). To date, binding sites of several protein–ligand complexes [11–17], including α-synuclein-spermine [15], adenylate kinase-ATP [16], and anterior gradient-2-PTTIYY hexapeptide interactions [17], were identified using this approach.

In order for such a top-down approach to be effective for ligand localization, there must be extensive fragmentation of the protein–ligand complex ions in the gas phase. One of the limitations of the electron-mediated dissociation methods is the low efficiency of the electron transfer/capture processes [12, 17–22]. Because electron capture cross sections increase quadratically with charge state, the efficiency of the process can be improved by increasing the charge state of the gaseous complex [12]. As shown by a number of different laboratories, the charge states of proteins and protein complexes in ESI can be significantly increased through the use of so-called "supercharging reagents", such as 3-nitrobenzoic acid (m-NBA) and sulfolane [23–27]. The mechanisms responsible for enhanced charging induced by supercharging agents have been extensively studied [23–29]. In a recent review, Loo and coworkers concluded that efficient positive ion supercharging reagents must be weak Brønsted bases, soluble in aqueous solution and be less (or similarly) volatile as the solvent [30]. They also advanced the hypothesis that high concentrations of the supercharging reagent in the ESI progeny droplets reduce the extent of acidic residue ionization, which effectively results in an increase in the protonation state of the gaseous protein ions [30].

While there have been many reported examples of protein supercharging in ESI-MS, there have been relatively few studies of the effects of supercharging agents on the structures and stabilities of multiprotein and protein–ligand complexes. Loo and coworkers reported that the supercharging of several protein–ligand and multiprotein complexes using m-NBA was accompanied with little or no change their native structures and noncovalent interactions [24]. More recently, it was shown by the same group that the use of sulfolane in reactive liquid sample desorption ESI (DESI)-MS can produce supercharging without destabilizing protein−ligand complexes [31]. However, studies have also shown that the structures and interactions of other protein complexes are susceptible to supercharging agents. For example, heme loss from myoglobin was observed upon addition of m-NBA or sulfolane to solution [25–27].

The goal of the present study is to investigate the influence of sulfolane on ESI-MS measurements of protein–ligand affinities in vitro. With this in mind, ESI-MS binding measurements were carried out on four protein–carbohydrate complexes in the presence and absence of sulfolane. The interactions between lysozyme (Lyz) and the tetrasaccharide ligand β-D-GlcNAc-(1→4)-β-D-GlcNAc-(1→4)-β-D-GlcNAc-(1→4)-D-GlcNAc (**L1**), a single chain variable fragment (scFv) of the monoclonal antibody Se155-4 and the trisaccharide ligand α-D-Gal-(1→2)-[α-D-Abe-(1→3)]-α-D-Man-OCH$_3$ (**L2**), cholera toxin B subunit homopentamer and the GM1 pentasaccharide β-D-Gal-(1→3)-β-D-GalNAc-(1→4)-[α-D-Neu5Ac-(2→3)]- β-D-Gal-(1→4)-β-D-Glc (**L3**), and a fragment of galectin 3 and the pentasaccharide ligand α-L-Fuc-(1→2)-β-D-Gal-(1→3)-β-D-GlcNAc-(1→3)-β-D-Gal-(1→4)-β-D-Glc (**L4**) served as model systems for this study. Having found evidence that sulfolane generally reduces the apparent affinity, a detailed study of the origin of the reduced affinity was undertaken using the Lyz–**L1** interaction as a model. Measurements were carried out using isothermal titration calorimetry (ITC), circular dichroism (CD), and nuclear magnetic resonance (NMR) spectroscopy to establish how sulfolane affects the structure and stability of the protein–tetrasaccharide complex in solution. Finally, the effect of sulfolane on protein–ligand affinity measurements carried out using liquid sample DESI-MS was explored.

Experimental

Materials

Ubiquitin (Ubq, MW 8565 Da), lysozyme from chicken egg white (Lyz, MW 14310 Da), cholera toxin B subunit homopentamer from *Vibrio cholera* (CTB$_5$, MW 58 kDa) were purchased from Sigma-Aldrich Canada (Oakville, Canada). The C-terminal fragment (residues 107-250) of human galectin-3 (Gal-3C, MW 16340 Da) and single chain variable fragment (scFv, MW 26539 Da) of the monoclonal antibody Se155-4 were produced and purified as described previously [32, 33]. The tetrasaccharide **L1** (MW 830.3 Da) was purchased from Dextra Science and Technology Centre (Reading, UK); the trisaccharide **L2** (MW 486.5 Da) was a gift from Professor D. Bundle (University of Alberta); the GM1 pentasaccharide **L3** (MW 998.3 Da) was purchased from HyTest Ltd. (Turku, Finland), and the pentasaccharide **L4** (MW 854.6 Da) was purchased from IsoSep AB (Tullinge, Sweden). Stock solutions of each protein (in 200 mM ammonium acetate) and each oligosaccharide (in deionized water) were prepared and stored at −20°C until needed.

Mass Spectrometry

A Synapt G2 quadrupole-ion mobility separation-time-of-flight (Q-IMS-TOF) mass spectrometer (Waters UK Ltd., Manchester, UK) with an 8 k quadrupole mass filter and a Synapt G2S Q-IMS-TOF mass spectrometer (Waters, Manchester, UK) with a 32 k quadrupole mass filter were used for ESI-MS and liquid sample DESI-MS measurements. Both instruments were equipped with nanoflow ESI (nanoESI) sources, which were operated in positive ion mode. NanoESI tips (~5 μm i.d.) were produced from borosilicate capillaries (1.0 mm o.d., 0.68 mm i.d.), using a P-1000 micropipette puller (Sutter Instruments, Novato, CA, USA). A capillary voltage of 1.0–1.3 kV was applied to a platinum wire to initiate the spray

on the Synapt G2 instrument, where the platinum wire was inserted into the nanoESI tip, and a capillary voltage of between 0.8 and 1.0 kV was applied to the Synapt G2S instrument. In both instruments, the cone voltage was maintained at 30 V and the source block temperature was 60°C. The trap and transfer collision energies were 5 and 2 V, respectively, and the argon pressures in the trap and transfer regions were 8.56×10^{-3} mbar and 8.62×10^{-3} mbar, respectively, for the Synapt G2S and 9.17×10^{-3} mbar and 9.28×10^{-3} mbar, respectively, for the Synapt G2. For the liquid sample DESI-MS measurements, a modified OMNI SPRAY ion source 2-D OS-6205 (Prosolia Inc., Indianapolis, IN, USA) was used. Details of the experimental setup can be found elsewhere [34]. Briefly, the liquid sample solution was delivered through a silica capillary (360 nm o.d., 100 nm i.d.) at a flow rate of 15 µL h^{-1} using a syringe pump. The outlet of the sample capillary was located between the ESI spray tip and the inlet to the mass spectrometer. The ESI solution flow rate was 2–3 µL min^{-1}. Capillary and cone voltages of 3.5 kV and 30 V, respectively, were used and the pressure of the N$_2$ nebulizing gas was 65 psi. The source block temperature was the same as for the ESI-MS binding measurements. All data were processed using MassLynx software (v4.1).

Isothermal Titration Calorimetry

The ITC affinity measurements performed on the Lyz–L1 interaction were carried out using a VP-ITC (MicroCal, Inc., Northampton, MA, USA). For each ITC experiment, the Lyz solution (0.2 mM) in the sample cell was titrated with a solution of L1 (2 mM); both the Lyz and L1 solutions were aqueous ammonium acetate (50 mM, pH 6.8, 25°C) containing varying percentages of sulfolane (2%, 5%, or 10%).

Circular Dichroism

Circular dichroism (CD) spectra were recorded at 25°C on an OLIS DSM CARY-17 spectrophotometer conversion and circular dichroism module (On-Line Instrument Systems Inc., Bogart, GA, USA) using a 0.2 mm path length quartz cuvette. Protein solutions (56 µM) were prepared in phosphate buffer (20 mM, pH 7.0) and varying percentages of sulfolane (0% to 20%). Data were collected in scanning mode from 250 to 190 nm and the average value of five repetitions was reported. Data were analyzed with OLIS Spectral Works (v4.3) and converted into molar ellipticity units. For each solution, the CD spectrum of the solvent alone was subtracted from the sample spectrum.

NMR Spectroscopy

All NMR spectra were acquired at 27°C on a 700 MHz Agilent/Varian spectrometer equipped with a cold probe (Agilent Technologies Inc., CA, USA). 1D ^{1}H and TROESY [35] NMR spectra were obtained for L1 in D$_2$O and in 2% (v/v) sulfolane–D$_2$O. The spectra were referenced to an external standard of acetone (2.22 ppm for ^{1}H), and the intensity of the residual HOD peak was decreased using a presaturation

pulse sequence, irradiating at 4.76 ppm. The spectral window was 8389 Hz (from 10.76 to –1.22 ppm). The 1D ^{1}H spectra were acquired in 16 transients, and no window functions were applied in the Fourier transformation. The TROESY spectra were acquired with eight transients in F2, 256 increments in F1, and a mixing time of 0.4 s. Sine-bell functions were applied interactively to improve signal-to-noise in the TROESY, but no line-broadening was used.

Natural abundance ^{1}H–^{15}N gHSQC NMR spectra were obtained for Lyz and Lyz–L1 complex in 10% (v/v) D$_2$O–H$_2$O with varying concentrations of sulfolane, 0%, 2%, 5%, and 10% (v/v). The Lyz concentration was 5 mM, and the L1 concentration was 20 mM. The spectra were acquired in a 5 mm D$_2$O-matched Shigemi tube at 27°C on a 700 MHz Agilent/Varian spectrometer equipped with a cold probe and referenced using the default parameters in the VNMR software. The spectral window for ^{1}H was 8389 Hz (from 10.71 to –1.26 ppm), and the spectral window for ^{15}N was 3545 Hz (139.8 to 90.2 ppm). The spectra were acquired with 16 transients in F2, 64 increments in F1, except for Lyz in 10% D$_2$O–H$_2$O, which was acquired with 76 increments in F1. The proton signals were decoupled during acquisition, and a $^1J_{N,H}$ value of 90 Hz was used. Sine-bell functions were applied interactively to improve signal-to-noise, but no line-broadening was used. An additional ^{1}H–^{15}N gHSQC NMR spectrum was acquired for denatured Lyz in 8 M urea and 10% (v/v) D$_2$O–H$_2$O. This spectrum was acquired in a 3 mm NMR tube, with 128 transients in F2 and 64 increments in F1. The remaining parameters were the same as for the folded protein.

Data Analysis

Average Charge State Calculation

The average charge state (*ACS*) of the protein–ligand complexe ions was calculated from the ESI mass spectrum using Equation 1:

$$ACS = \frac{\sum_n [Ab(\text{PL}^{n+}) \times n]}{\sum_n Ab(\text{PL}^{n+})} \qquad (1)$$

where $Ab(\text{PL}^{n+})$ is the abundance of the protein–ligand complex ions and n is the charge state. The *ACS* of the protein ions was calculated in the same way.

Association Constants from ESI Mass Spectra

The general procedure for determining association constants (K$_a$) for protein–ligand interactions from ESI mass spectra has been described in detail elsewhere [34, 36–38] and only a brief description is given for the case where the protein has a single ligand binding site. The assay relies on the detection and quantification of the gas-phase ions of the free and ligand-bound protein. Following correction of the mass spectrum for the occurrence of nonspecific ligand-protein binding during the

ESI process using the reference protein method [37, 38], the ratio (R) of the total abundance (Ab) of ligand-bound protein (PL) to free protein (P) ions is taken to be equal to the concentration ratio of PL to P, Equation 2:

$$R = \frac{\sum Ab(\text{PL})}{\sum Ab(\text{P})} = \frac{[\text{PL}]}{[\text{P}]} \tag{2}$$

and K_a calculated from Equation 3:

$$K_a = \frac{R}{[\text{L}]_0 - \dfrac{R}{1+R}[\text{P}]_0} \tag{3}$$

where $[\text{P}]_0$ and $[\text{L}]_0$ are the initial protein and ligand concentrations, respectively. Details on the determination of K_a for the stepwise binding of **L3** to CTB$_5$ [39, 40] are given in Supplementary Data.

Results and Discussion

Influence of Sulfolane on Protein–Carbohydrate Affinities

Direct ESI-MS Binding Measurements ESI-MS binding measurements were carried out on four protein–carbohydrate complexes to assess whether protein–ligand interactions are generally influenced by the presence of sulfolane in solution. Shown in Figures 1 and 2 are representative ESI mass spectra acquired in positive ion mode for aqueous ammonium acetate solutions (50 mM, pH 6.8, and 25°C) containing each protein/carbohydrate ligand pair in the absence and presence of sulfolane (H$_2$O:sulfolane 98:2 v/v). A reference protein (P$_{\text{ref}}$) was added to each solution in order to identify the occurrence of nonspecific carbohydrate-protein binding during the ESI process [37, 38].

Inspection of the mass spectrum measured for a solution of Lyz (10 µM), **L1** (15 µM), and P$_{\text{ref}}$ (Ubq, 5 µM) reveals the presence of protonated Lyz^{n+} and (Lyz + **L1**)$^{n+}$ ions, at n = 7 and 8, together with Ubq^{n+} ions at n = 5 and 6 (Figure 1a). The absence of (P$_{\text{ref}}$ + **L1**)$^{n+}$ ions indicates that nonspecific binding was negligible under these experimental conditions. From the ratio of the total abundance of (Lyz + **L1**)$^{n+}$ to Lyz^{n+} ions and the known initial concentrations, a K_a value of $(7.6 \pm 0.2) \times 10^4\,\text{M}^{-1}$ was determined from the mass spectrum (Equations 2 and 3). This value is in reasonable agreement with previously reported values, $0.8–1.1 \times 10^5\,\text{M}^{-1}$ [34, 41, 42]. Upon addition of 2% sulfolane to the solution, the charge states of the Lyz^{n+} and (Lyz + **L1**)$^{n+}$ ions shifted to n = 8–12 (Figure 1b). This shift corresponds to an increase of 35% in *ACS* for the (Lyz + **L1**)$^{n+}$ ions; the Lyz^{n+} ions exhibited a similar increase in *ACS* (~40% increase). The P$_{\text{ref}}$$^{n+}$ ions also shifted to higher charges states, n = 6 to 10, which corresponds to a 50% increase in *ACS*. Also evident in the mass spectrum are Lyz^{n+} and (Lyz + **L1**)$^{n+}$ ions bound to one or more sulfolane molecules. Similar observations have been reported for other proteins analyzed in the presence of
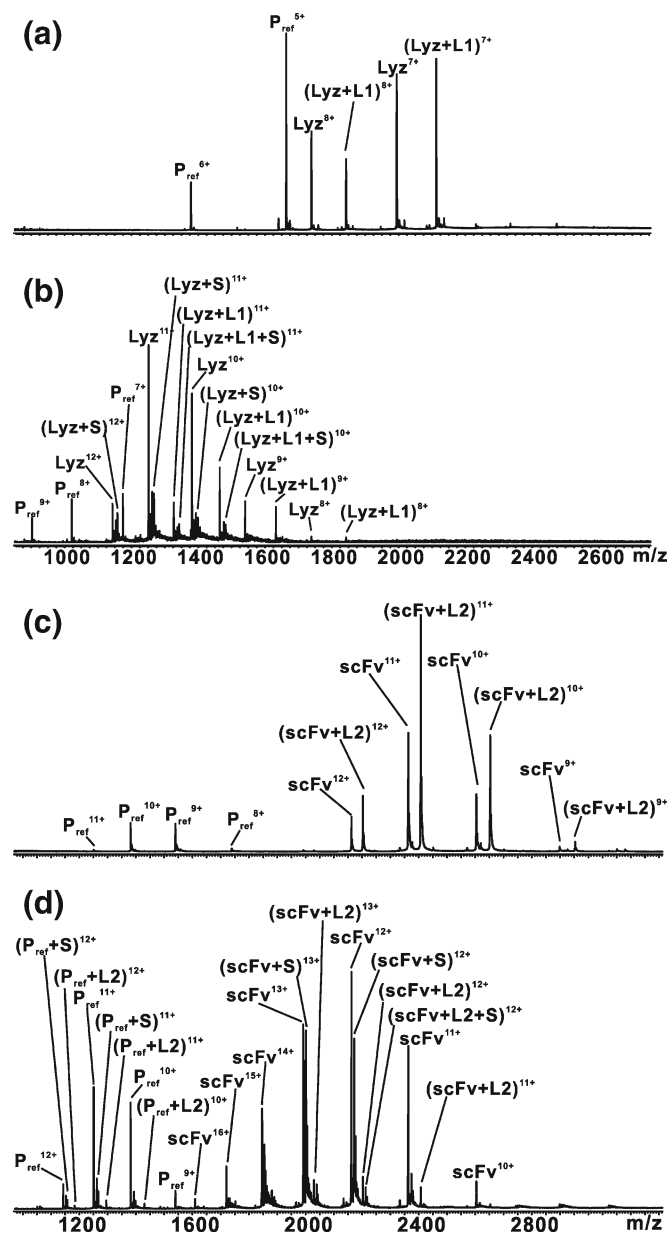
Figure 1. Representative ESI mass spectra acquired in positive ion mode for aqueous ammonium acetate (50 mM) solutions of Lyz (10 µM), **L1** (15 µM), and P$_{\text{ref}}$ (Ubq, 5 µM) with **(a)** 0% sulfolane and **(b)** 2% sulfolane, or scFv (10 µM), **L2** (15 µM), and P$_{\text{ref}}$ (Lyz, 5 µM), with **(c)** 0% sulfolane and **(d)** 2% sulfolane. Nonspecific sulfolane adducts are labeled as "S"

sulfolane by ESI-MS [43]. Notably, there is a significant reduction in the abundance of (Lyz + **L1**)$^{n+}$ ions, relative to Lyz^{n+} ions; the measured K_a is $(4.1 \pm 0.1) \times 10^4\,\text{M}^{-1}$, which corresponds to a 46% decrease in affinity compared with the value measured for the same solution but in the absence of sulfolane.

Analogous measurements were carried out on solutions with up to 10% sulfolane. Plotted in Figure 3 are the *ACS* values determined for the (Lyz + **L1**)$^{n+}$ ions and the corresponding K_a values measured for the solutions at different percentages of sulfolane. It can be seen that the dependence
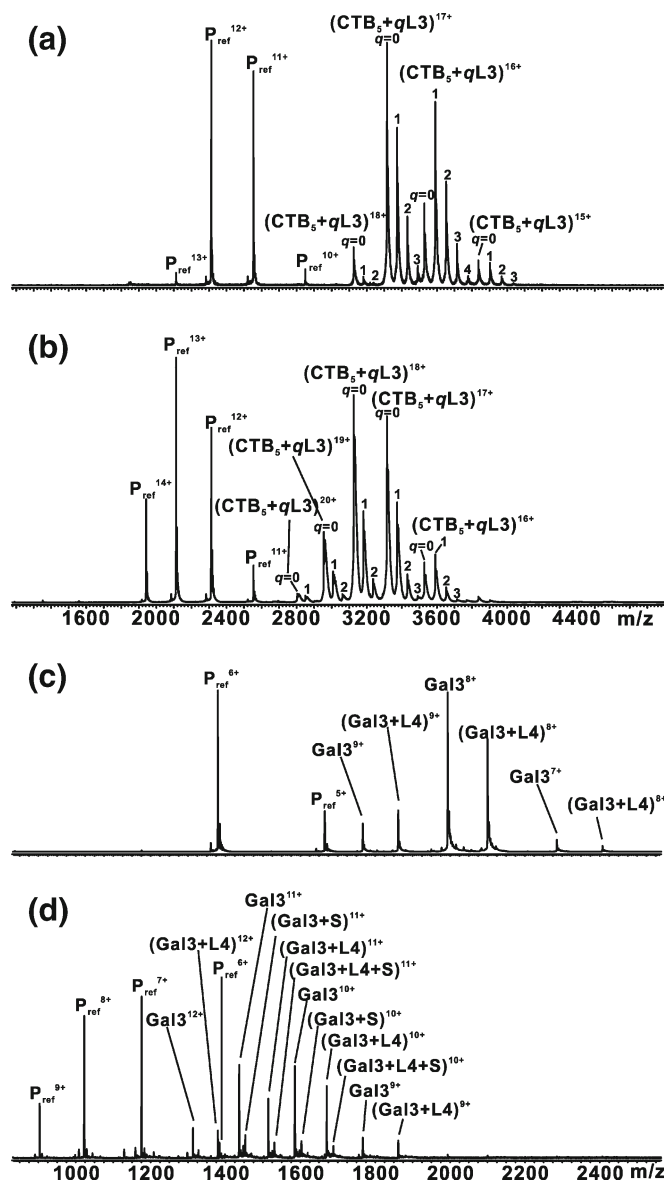
Figure 2. Representative ESI mass spectra acquired in positive ion mode for aqueous ammonium acetate (50 mM) solutions of CTB_5 (5 µM), **L3** (5 µM), and P_{ref} (scFv, 3 µM) with **(a)** 0% sulfolane and **(b)** 2% sulfolane, or Gal3-C (10 µM), **L4** (10 µM), and P_{ref} (Ubq, 5 µM) with **(c)** 0% sulfolane and **(d)** 2% sulfolane. Nonspecific sulfolane adducts are labelled as "S"

of *ACS* on sulfolane concentration is most pronounced up to ~2% sulfolane; at higher concentrations, only a slight increase in *ACS* was observed, reaching a value of (10.93 ± 0.01) at 10% sulfolane. The dependence of K_a is also most pronounced at the lower concentrations of sulfolane, but the affinity continues to decrease with increasing sulfolane concentrations, dropping to $(5.5 ± 0.3) \times 10^3$ M^{-1} at 10% sulfolane. This change in K_a corresponds to a 93% decrease in affinity.

The results obtained for the scFv–**L2**, CTB_5–**L3**, and Gal3C–**L4** interactions are qualitatively similar to those described above for the Lyz–**L1** system. Shown in Figure 1c and d are the ESI mass spectra for a solution of scFv (10 µM), **L2** (10 µM), and P_{ref} (Lyz, 5 µM), in the absence and presence of sulfolane, respectively. In the absence of sulfolane,

protonated $scFv^{n+}$ and $(scFv + **L2**)^{n+}$ ions, at n = 9 to 12, together with P_{ref}^{n+} ions at n = 8 to 11, were detected. The measured K_a value for the (scFv + **L2**) complex, $(8.2 ± 0.1) \times 10^4$ M^{-1}, is in good agreement with the reported values, which are in the $0.66–1.2 \times 10^5$ M^{-1} range [34, 44]. Upon addition of sulfolane, the *ACS* of the $scFv^{n+}$ and $(scFv + **L2**)^{n+}$ ions increased by ~14% and the presence of sulfolane adducts was evident. The measured K_a, $(2.9 ± 0.1) \times 10^3$ M^{-1}, is 96% smaller than the value $[(8.2 ± 0.1) \times 10^4$ $M^{-1}]$ measured in the absence of sulfolane. Shown in Figure 2a and b are representative ESI mass spectra for a solution of CTB_5 (5 µM), **L3** (5 µM), and P_{ref} (scFv, 3 µM) in the absence and presence of sulfolane, respectively. In the absence of sulfolane, protonated CTB_5^{n+} and $(CTB_5 + q**L3**)^{n+}$ ions, where q = 1–4, at n = 15–18 are detected,
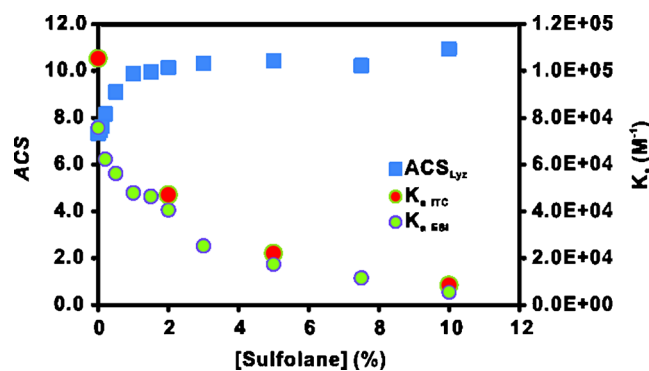
Figure 3. Plot of average charge state (*ACS*) of the (Lyz + **L1**) ions observed from ESI mass spectra acquired for aqueous ammonium acetate (50 mM) solutions of Lyz (10 μM), **L1** (15 μM), and Ubq (5 μM) with 0%–10% sulfolane. Also shown are the association constants (K_a) for the (Lyz + **L1**) interaction measured by ESI-MS and isothermal titration calorimetry (ITC)

along with P_{ref}^{n+} ions at n = 10–13. The association constants for the stepwise binding (i.e., $K_{a,q}$) of three molecules of **L3** to CTB_5 [$(1.5 \pm 0.1) \times 10^7 \, M^{-1}$ ($K_{a,1}$), $(8.1 \pm 0.1) \times 10^6 \, M^{-1}$ ($K_{a,2}$), and $(5.4 \pm 0.1) \times 10^6 \, M^{-1}$ ($K_{a,3}$)] are consistent with reported values ($K_{a,1} = 1.6 \times 10^7 \, M^{-1}$, $K_{a,2} = 7.3 \times 10^6 \, M^{-1}$, and $K_{a,3} = 3.8 \times 10^6 \, M^{-1}$) [40]. Upon addition of sulfolane, the *ACS* of the CTB_5^{n+} and $(CTB_5 + q\mathbf{L3})^{n+}$ ions increased by ~6%, whereas the $K_{a,q}$ values decreased by 98% [$(2.6 \pm 0.1) \times 10^5 \, M^{-1}$ ($K_{a,1}$), $(1.3 \pm 0.1) \times 10^5 \, M^{-1}$ ($K_{a,2}$), and $(1.1 \pm 0.1) \times 10^5 \, M^{-1}$ ($K_{a,3}$)]. ESI mass spectra measured for a solution of Gal3C (10 μM), **L4** (10 μM), and P_{ref} (Ubq, 6 μM), in the absence and presence of sulfolane are shown in Figure 2c and d, respectively. In the absence of sulfolane, protonated $Gal3C^{n+}$ and $(Gal3C + \mathbf{L4})^{n+}$ ions, at n = 7 to 9, together with P_{ref}^{n+} ions at n = 5 to 6, were detected. The measured K_a, $(1.45 \pm 0.02) \times 10^5 \, M^{-1}$, is similar to the reported value, $2 \times 10^5 \, M^{-1}$ [45]. The introduction of sulfolane to the solution resulted in an increase of 28% in the *ACS* of the $Gal3C^{n+}$ and $(Gal3C + \mathbf{L4})^{n+}$ ions; sulfolane adducts were also observed. The K_a, $(1.25 \pm 0.02) \times 10^5 \, M^{-1}$, is ~14% lower than the value measured in the absence of sulfolane [$(1.45 \pm 0.02) \times 10^5 \, M^{-1}$].

The present results suggest that protein–carbohydrate affinities measured by ESI-MS are generally sensitive to the presence of sulfolane, and that the magnitude of the reduction in affinity (at a given sulfolane concentration) is dependent on the nature of the protein–carbohydrate interactions. However, it is not clear from the ESI-MS data alone whether this effect occurs in bulk solution, during the ESI process, or as a result of in-source (gas-phase) dissociation. With the goal of establishing the origin(s) of the reduced affinity (as measured by ESI-MS), ITC measurements, CD spectroscopy, and NMR spectroscopy experiments were used to quantify the Lyz–**L1** interaction in the absence and presence of sulfolane and to establish whether the sulfolane influences the higher order structure

of Lyz or the Lyz–**L1** complex in solution, or interacts strongly with **L1** or Lyz.

Influence of Sulfolane on the (Lyz + L1) Complex in Solution.

Isothermal titration calorimetry was used to quantify the effect of sulfolane on the stability of the (Lyz + **L1**) complex in solution. Binding measurements were carried out for aqueous solutions of Lyz (0.2 mM) and **L1** (2.0 mM) with 2%, 5%, and 10% sulfolane, respectively (Figures S1, S2, and S3, Supplementary Data). Plotted in Figure 3 are the corresponding K_a values as well as the reported value measured in the absence of sulfolane [34], together with the values measured by ESI-MS. Notably, the ITC data reveal that sulfolane reduces the thermodynamic stability of the Lyz–**L1** interaction in solution. Moreover, the K_a values measured by ESI-MS are in good agreement with the values determined by ITC. This finding confirms that ESI-MS provides an accurate measure of the distribution of free and **L1**-bound Lyz in the sulfolane-containing solutions, which implies that the (Lyz + **L1**) complex does not dissociate during the ESI process or in the gas phase (i.e., in-source dissociation).

The decrease in K_a upon introduction of sulfolane to solution could be due to changes in higher-order structure of Lyz or due to general or specific solvent effects. CD spectroscopy was employed to assess whether the addition of sulfolane alters the secondary structure of Lyz, which contains five standard alpha helical regions, five β-pleated sheet regions, and four disulfide bonds [46]. Shown in Figure S4 (Supplementary Data) are CD spectra measured for solutions of Lyz (56 μM) and sulfolane (0%–20%) in phosphate buffer (20 mM, pH 7, 25°C). CD spectra of Lyz in solutions with different concentrations of sulfolane did not show significant change in the 190–250 nm region [47–49]. The results from CD experiments suggested that sulfolane does not significantly influence the secondary structure of Lyz in bulk solution. This is consistent with the findings of Klibanov and co-workers, who previously reported that Lyz is resistant to significant structural changes in the presence of high concentrations [up to 60% (v/v)] of organic solvents (e.g., acetonitrile, tetrahydrofuran, and 1-propanol) [50].

To gain further insight into the origin of the reduced affinity resulting from the addition to sulfolane, solution NMR experiments were performed on Lyz, **L1**, and the (Lyz + **L1**) complex, in the absence and presence of sulfolane [0%–10%, (v/v)] to identify any structural changes in Lyz or the (Lyz + **L1**) complex. Natural abundance ^1H–^{15}N gHSQC NMR spectra for Lyz in 10% (v/v) D_2O–H_2O and with varying concentrations of sulfolane [0%, 2%, 5%, and 10% (v/v)] are shown in Figures S5 and S6 (Supplementary Data), respectively. Backbone NH signals for Lyz were assigned based on comparisons with literature values [51, 52]. The addition of sulfolane does not cause major changes in the ^{15}N chemical shifts of the backbone NH peaks (Figure S6, Supplementary Data), and Lyz remains

folded at sulfolane concentrations of up to 10% (Figures S6 and S7, Supplementary Data). Notably, the resonances with the largest ^{1}H chemical shift changes—R5, A42, S50, C80, S81, S100, N106, W108, K116, A122, L124, R128—are not part of the **L1** binding site [53–55].

Alternatively, the reduced affinity could be due to interactions between sulfolane and **L1** or the (Lyz + **L1**) complex. ^{1}H NMR spectra of **L1** in D_2O and in 2% (v/v) sulfolane–D_2O are shown in Figure S8 (Supplementary Data). None of the chemical shifts or coupling constants for the **L1** change with the addition of sulfolane, which indicates sulfolane does not form any strong interactions with **L1**. To determine whether the addition of sulfolane affects the conformation of **L1**, TROESY spectra [35] were acquired in both solvent systems. The signals for **L1** are unchanged in both spectra (Figure S9, Supplementary Data), and there are no cross peaks between **L1** and sulfolane, which means sulfolane does not change the conformation of **L1** in solution. Natural abundance ^{1}H–^{15}N gHSQC NMR spectra for the (Lyz + **L1**) complex in 10% (v/v) D_2O–H_2O and with varying concentrations of sulfolane [0%, 2%, 5, and 10% (v/v)] are shown in Figures S10 and S11 (Supplementary Data), respectively. The spectra for Lyz with and without **L1** are very similar (Figure S10, Supplementary Data), as expected because the structure of Lyz changes very little upon ligand binding [56]. Three new signals are observed for the amide groups in **L1** [57]. The addition of sulfolane to the (Lyz + **L1**) complex causes similar changes in the spectra to those observed for Lyz alone (compare Figures S6 and S11, Supplementary Data).

Taken together, the results of the ITC, CD, and NMR spectroscopy measurements reveal that the reduction in the affinity of the (Lyz + **L1**) complex induced by sulfolane is not the result of significant change in protein conformation, nor

from solvent effects related to sulfolane interactions with **L1** or Lyz residues located in the binding pocket. Consequently, it would seem that loss of affinity is related to a general solvent effect, whereby sulfolane increases the energetic penalty associated with solvent reorganization of the **L1** and Lyz required for binding. That the addition of sulfolane to aqueous solutions affects the hydrogen bonding network of water provides indirect support for this hypothesis [58].

Supercharging and Liquid Sample DESI-MS

Recently, it was shown that liquid sample and reactive liquid sample DESI-MS can be used to quantify protein–-ligand affinities in solution [31, 34]. An attractive feature of the liquid sample DESI-MS assay is that it is significantly more tolerant to nonvolatile buffers, such as PBS, than ESI-MS [31, 34]. With this feature in mind, the application of liquid sample DESI-MS for protein–ligand affinity measurements carried out in the presence of supercharging reagents was investigated. In these experiments, the "sample solution" contained Lyz, **L1**, and P_{ref} in 50 mM aqueous ammonium acetate, whereas the "ESI solution" contained either $ACN:H_2O$ (50:50, v/v) or $ACN:H_2O:sulfolane$ (49.75:49.75:0.5, v/v). Shown in Figure 4a and b are representative liquid sample DESI mass spectra for a sample solution of Lyz (10 μM), **L1** (15 μM), and P_{ref} (Ubq, 5 μM), measured in the absence and presence of sulfolane, respectively. It can be seen that the ACS for Lyz^{n+} and $(Lyz + **L1**)^{n+}$ ions increased by ~20% in the presence of sulfolane, which is similar to ~24% increase of ESI-MS measurements acquired using 0.5% sulfolane. Overall, however, the ACS of Lyz and (Lyz + **L1**) complex in the presence and absence of sulfolane on liquid sample DESI spectra were lower
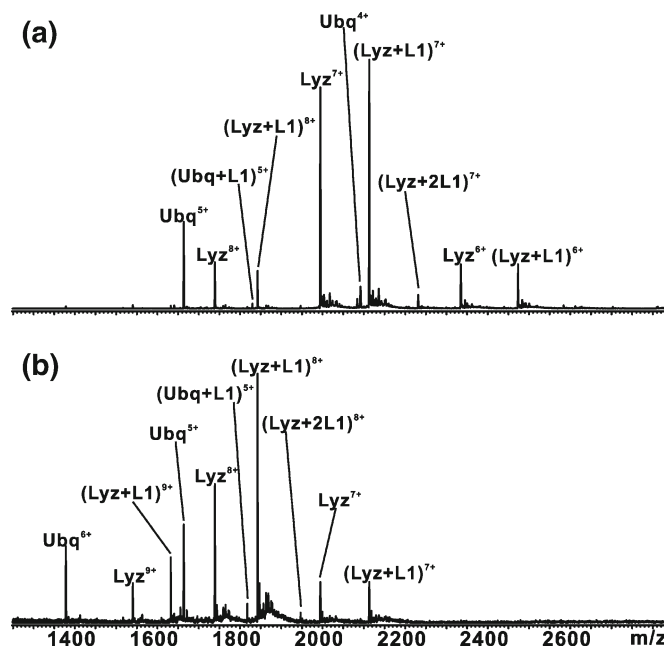
Figure 4. Liquid sample DESI mass spectra acquired in positive ion mode for aqueous ammonium acetate (20 mM) solutions of Lyz (10 μM), **L1** (15 μM), and Ubq (5 μM) using an ESI spray solvent (ACN:H_2O = 50:50, v/v) containing **(a)** 0% Sulfolane and **(b)** 0.5% sulfolane

than the *ACS* observed on their corresponding ESI spectra when the same solutions were sprayed. The lower *ACS* observed in the DESI spectra, which is consistent with the results of previous studies [58–60], may be due to the presence of ACN vapor in the source region. Acetonitrile has a higher gas-phase basicity (178.8 kcal mol^{-1}) than H_2O (157.9 kcal mol^{-1}) [61], and would more efficiently deprotonate the Lyz ions in the source compared to H_2O vapor.

Notably, and in contrast to what was observed with ESI-MS, there is no measurable change in the K_a value for this interaction upon addition of sulfolane [$(1.1 \pm 0.1) \times 10^5$ M^{-1} (0% sulfolane) and $(1.4 \pm 0.1) \times 10^5$ M^{-1} (0.5% sulfolane)]. This finding, which is consistent with observations mde by Loo and coworkers [31], is significant in that it reveals that protein supercharging and the reduction in the K_a of the (Lyz + **L1**) complex caused by sulfolane are independent processes. The absence of a change in the distribution of bound and unbound Lyz in liquid sample DESI-MS can reasonably be explained on the basis of the limited time available for re-equilibration of the Lyz-**L1** interaction upon introduction of sulfolane into the droplet. In fact, it was reported recently that using liquid sample DESI-MS implemented with **L1** in the ESI spray solution and Lyz in the sample solution, the lifetime of the resulting droplets (containing sample) was too short for the Lyz-**L1** interaction to reach equilibrium [34]. That supercharging is observed in the liquid sample DESI-MS measurements carried out with sulfolane demonstrates that the process involved in supercharging occur on a much shorter timescale than the relaxation kinetics for the Lyz–**L1** interaction.

Conclusions

The results of quantitative ESI-MS binding measurements performed on four protein–carbohydrate interactions (Lyz-**L1**, scFv-**L2**, CTB$_5$-**L3**, and Gal3C-**L4**) revealed that using sulfolane to supercharge protein ions is generally accompanied by a reduction in ligand affinity, although the magnitude of the effect (at a given sulfolane concentration) is dependent on the nature of the interaction. The affinities measured by ESI-MS for the Lyz-**L1** interaction in the presence of sulfolane agree with values measured by ITC. This finding indicates that there is no dissociation of the complex during the ESI process (i.e., in the droplets) or in the gas phase (i.e., in-source dissociation). Moreover, the results of CD and NMR spectroscopy measurements reveal that sulfolane does not cause any significant change in the higher order structure of Lyz, nor does it interact strongly with **L1** or the Lyz residues that make up the binding pocket in solution. It is proposed that sulfolane weakens the protein–ligand interactions through a general solvent effect. Taken together, the present findings suggest that supercharging of the (Lyz + **L1**) complex by sulfolane is not related to changes to protein structure in bulk solution or during the ESI process. It must be stressed, though, that the possibility of sulfolane-induced protein unfolding in the ESI droplets can not be definitively ruled out based on the current results. However, if protein unfolding does

take place during the ESI process, the unfolding kinetics must be significantly faster than the dissociation kinetics. Finally, binding measurements performed on the Lyz-**L1** interaction using liquid sample DESI-MS revealed that the introduction of sulfolane into the ESI solution results in protein supercharging; however, this effect is not accompanied by any loss in affinity. This finding, in addition to having mechanistic implications, suggests an inherent advantage of liquid sample DESI-MS over direct ESI-MS for protein-ligand affinity measurements in cases where supercharging is desirable.

Acknowledgments

References

1. Cubrilovic, D., Biela, A., Sielaff, F., Steinmetzer, T., Klebe, G., Zenobi, R.: Quantifying Protein-ligand binding constants using electrospray ionization mass spectrometry: a systematic binding affinity study of a series of hydrophobically modified trypsin inhibitors. J. Am. Soc. Mass Spectrom. **23**, 1768–1777 (2012)

2. El-Hawiet, A., Shoemaker, G.K., Daneshfar, R., Kitova, E.N., Klassen, J.S.: Applications of a catch and release electrospray ionization mass spectrometry assay for carbohydrate library screening. Anal. Chem. **84**, 50–58 (2011)

3. Han, L., Kitov, P.I., Kitova, E.N., Tan, M., Wang, L., Xia, M., Jiang, X., Klassen, J.S.: Affinities of recombinant norovirus p dimers for human blood group antigens. Glycobiology **23**, 276–285 (2013)

4. Kitova, E.N., El-Hawiet, A., Klassen, J.S.: Screening carbohydrate libraries for protein interactions using the direct esi-ms assay. Applications to libraries of unknown concentration. J. Am. Soc. Mass Spectrom. **25**, 1908–1916 (2014)

5. Kitova, E.N., Bundle, D.R., Klassen, J.S.: Thermal dissociation of protein–oligosaccharide complexes in the gas phase: mapping the intrinsic intermolecular interactions. J. Am. Chem. Soc. **124**, 5902–5913 (2002)

6. Kitova, E.N., Bundle, D.R., Klassen, J.S.: Partitioning of solvent effects and intrinsic interactions in biological recognition. Angew. Chem. Int. Ed. **43**, 4183–4186 (2004)

7. Liu, L., Bagal, D., Kitova, E.N., Schnier, P.D., Klassen, J.S.: Hydrophobic protein−ligand interactions preserved in the gas phase. J. Am. Chem. Soc. **131**, 15980–15981 (2009)

8. Liu, L., Michelsen, K., Kitova, E.N., Schnier, P.D., Klassen, J.S.: Evidence that water can reduce the kinetic stability of protein−hydrophobic ligand interactions. J. Am. Chem. Soc. **132**, 17658–17660 (2010)

9. Liu, L., Michelsen, K., Kitova, E.N., Schnier, P.D., Klassen, J.S.: Energetics of lipid binding in a hydrophobic protein cavity. J. Am. Chem. Soc. **134**, 3054–3060 (2012)

10. Deng, L., Broom, A., Kitova, E.N., Richards, M.R., Zheng, R.B., Shoemaker, G.K., Meiering, E.M., Klassen, J.S.: Kinetic stability of the streptavidin–biotin interaction enhanced in the gas phase. J. Am. Chem. Soc. **134**, 16586–16596 (2012)

11. Haselmann, K.F., Jørgensen, T.J.D., Budnik, B.A., Jensen, F., Zubarev, R.A.: Electron capture dissociation of weakly bound polypeptide polycationic complexes. Rapid Commun. Mass Spectrom. **16**, 2260–2265 (2002)

12. Yin, S., Loo, J.A.: Top-down mass spectrometry of supercharged native protein–ligand complexes. Int. J. Mass Spectrom. **300**, 118–122 (2011)

13. Jackson, S.N., Dutta, S., Woods, A.S.: The use of ECD/ETD to identify the site of electrostatic interaction in noncovalent complexes. J. Am. Soc. Mass Spectrom. **20**, 176–179 (2009)

14. Muller, L., Jackson, S.N., Woods, A.S.: ETD and sequential ETD localize the residues involved in D2-A2A heteromerization. RSC Adv **4**, 42272–42277 (2014)

15. Xie, Y., Zhang, J., Yin, S., Loo, J.A.: Top-down ESI-ECD-FT-ICR mass spectrometry localizes noncovalent protein-ligand binding sites. J. Am. Chem. Soc. **128**, 14432–14433 (2006)

16. Yin, S., Loo, J.A.: Elucidating the site of protein-ATP binding by top-down mass spectrometry. J. Am. Soc. Mass Spectrom. **21**, 899–907 (2010)

17. Clarke, D.J., Murray, E., Hupp, T., Mackay, C.L., Langridge-Smith, P.R.: Mapping a noncovalent protein-peptide interface by top-down FTICR mass spectrometry using electron capture dissociation. J. Am. Soc. Mass Spectrom. **22**, 1432–1440 (2011)

18. Ledvina, A.R., McAlister, G.C., Gardner, M.W., Smith, S.I., Madsen, J.A., Schwartz, J.C., Stafford Jr., G.C., Syka, J.E.P., Brodbelt, J.S., Coon, J.J.: Infrared photo-activation reduces peptide folding and hydrogen atom migration following ETD tandem mass spectrometry. Angew. Chem. Int. Ed. Engl. **48**, 8526–8528 (2009)

19. Swaney, D.L., McAlister, G.C., Wirtala, M., Schwartz, J.C., Syka, J.E.P., Coon, J.J.: Supplemental activation method for high-efficiency electron-transfer dissociation of doubly protonated peptide precursors. Anal. Chem. **79**, 477–485 (2007)

20. Horn, D.M., Breuker, K., Frank, A.J., McLafferty, F.W.: Kinetic intermediates in the folding of gaseous protein ions characterized by electron capture dissociation mass spectrometry. J. Am. Chem. Soc. **123**, 9792–9799 (2001)

21. Gorshkov, M.V., Masselon, C.D., Nikolaev, E.N., Udseth, H.R., Paša-Tolić, L., Smith, R.D.: Considerations for electron capture dissociation efficiency in FTICR mass spectrometry. Int. J. Mass Spectrom. **234**, 131–136 (2004)

22. Zenaidee, M.A., Donald, W.A.: Extremely supercharged proteins in mass spectrometry: profiling the ph of electrospray generated droplets, narrowing charge state distributions, and increasing ion fragmentation. Analyst **140**, 1894–1905 (2015)

23. Iavarone, A.T., Jurchen, J.C., Williams, E.R.: Supercharged protein and peptide ions formed by electrospray ionization. Anal. Chem. **73**, 1455–1460 (2001)

24. Lomeli, S.H., Yin, S., Ogorzalek Loo, R.R., Loo, J.A.: Increasing charge while preserving noncovalent protein complexes for ESI-MS. J. Am. Soc. Mass Spectrom. **20**, 593–596 (2009)

25. Sterling, H.J., Williams, E.R.: Origin of supercharging in electrospray ionization of noncovalent complexes from aqueous solution. J. Am. Soc. Mass Spectrom. **20**, 1933–1943 (2009)

26. Lomeli, S.H., Peng, I.X., Yin, S., Ogorzalek Loo, R.R., Loo, J.A.: New reagents for increasing ESI multiple charging of proteins and protein complexes. J. Am. Soc. Mass Spectrom. **21**, 127–131 (2010)

27. Sterling, H.J., Daly, M.P., Feld, G.K., Thoren, K.L., Kintzer, A.F., Krantz, B.A., Williams, E.R.: Effects of supercharging reagents on noncovalent complex structure in electrospray ionization from aqueous solutions. J. Am. Soc. Mass Spectrom. **21**, 1762–1774 (2010)

28. Iavarone, A.T., Williams, E.R.: Mechanism of charging and supercharging molecules in electrospray ionization. J. Am. Chem. Soc. **125**, 2319–2327 (2003)

29. Hogan Jr., C.J., Ogorzalek Loo, R.R., Loo, J.A., Fernández de la Mora, J.: Ion mobility-mass spectrometry of phosphorylase B ions generated with supercharging reagents but in charge-reducing buffer. Phys. Chem. Chem. Phys. **12**, 13476–13483 (2010)

30. Ogorzalek Loo, R.R., Lakshmanan, R.L., Loo, J.A.: What protein charging (and supercharging) reveal about the mechanism of electrospray ionization. J. Am. Soc. Mass Spectrom. **25**, 1675–1693 (2014)

31. Liu, P., Zhang, J., Ferguson, C.N., Chen, H., Loo, J.A.: Measuring protein–ligand interactions using liquid sample desorption electrospray ionization mass spectrometry. Anal. Chem. **85**, 11966–11972 (2013)

32. Zdanov, A., Li, Y., Bundle, D.R., Deng, S.J., MacKenzie, C.R., Narang, S.A., Young, N.M., Cygler, M.: Structure of a single-chain antibody variable domain (Fv) fragment complexed with a carbohydrate antigen at 1.7-A resolution. Proc. Natl. Acad. Sci. **91**, 6423–6427 (1994)

33. Rademacher, C., Shoemaker, G.K., Kim, H.-S., Zheng, R.B., Taha, H., Liu, C., Nacario, R.C., Schriemer, D.C., Klassen, J.S., Peters, T., Lowary, T.L.: Ligand specificity of CS-35, a monoclonal antibody that recognizes mycobacterial lipoarabinomannan: a model system for oligofuranoside–protein recognition. J. Am. Chem. Soc. **129**, 10489–10502 (2007)

34. Yao, Y., Shams-Ud-Doha, K., Daneshfar, R., Kitova, E.N., Klassen, J.S.: Quantifying protein–carbohydrate interactions using liquid sample desorption electrospray ionization mass spectrometry. J. Am. Soc. Mass Spectrom. **26**, 98–106 (2015)

35. Hwang, T.L., Shaka, A.J.: Cross relaxation without TOCSY: transverse rotating-frame overhauser effect spectroscopy. J. Am. Chem. Soc. **114**, 3157–3159 (1992)

36. Wang, W., Kitova, E.N., Klassen, J.S.: Influence of solution and gas phase processes on protein−carbohydrate binding affinities determined by nanoelectrospray fourier transform ion cyclotron resonance mass spectrometry. Anal. Chem. **75**, 4945–4955 (2003)

37. Wang, W., Kitova, E.N., Klassen, J.S.: Nonspecific Protein−Carbohydrate complexes produced by nanoelectrospray ionization. Factors influencing their formation and stability. Anal. Chem. **77**, 3060–3071 (2005)

38. Sun, J., Kitova, E.N., Wang, W., Klassen, J.S.: Method for distinguishing specific from nonspecific protein−ligand complexes in nanoelectrospray ionization mass spectrometry. Anal. Chem. **78**, 3010–3018 (2006)

39. Turnbull, W.B., Precious, B.L., Homans, S.W.: Dissecting the cholera toxin–ganglioside GM1 interaction by isothermal titration calorimetry. J. Am. Chem. Soc. **126**, 1047–1054 (2004)

40. Lin, H., Kitova, E.N., Klassen, J.S.: Measuring positive cooperativity using the direct ESI-MS assay. cholera toxin B subunit homopentamer binding to GM1 pentasaccharide. J. Am. Soc. Mass Spectrom. **25**, 104–110 (2014)

41. Schindler, M., Assaf, Y., Sharon, N., Chipman, D.M.: Mechanism of lysozyme catalysis: role of ground-state strain in subsite D in hen egg-white and human lysozymes. Biochemistry **16**, 423–431 (1977)

42. Veros, C.T., Oldham, N.J.: Quantitative determination of lysozyme-ligand binding in the solution and gas phases by electrospray ionisation mass spectrometry. Rapid Commun. Mass Spectrom. **21**, 3505–3510 (2007)

43. Douglass, K.A., Venter, A.R.: Investigating the role of adducts in protein supercharging with sulfolane. J. Am. Soc. Mass Spectrom. **23**, 489–497 (2012)

44. Daneshfar, R., Kitova, E.N., Klassen, J.S.: Determination of protein-ligand association thermochemistry using variable-temperature nanoelectrospray mass spectrometry. J. Am. Chem. Soc. **126**, 4786–4787 (2004)

45. Hirabayashi, J., Hashidate, T., Arata, Y., Nishi, N., Nakamura, T., Hirashima, M., Urashima, T., Oka, T., Futai, M., Muller, W.E.G., Yagi, F., Kasai, K.: Oligosaccharide specificity of galectins: a search by frontal affinity chromatography. Biochim. Biophys. Acta **1572**, 232–254 (2002)

46. Phillips, D.C.: The hen egg-white lysozyme molecule. Proc. Natl. Acad. Sci. **57**, 483–495 (1967)

47. Holzwarth, G., Doty, P.: The ultraviolet circular dichroism of polypeptides. J. Am. Chem. Soc. **87**, 218–228 (1965)

48. Greenfield, N., Fasman, G.D.: Computed circular dichroism spectra for the evaluation of protein comformation. Biochemistry **8**, 4108–4116 (1969)

49. Venyaminov, S., Baikalov, I.A., Shen, Z.M., Wu, C.S., Yang, J.T.: Circular dichroic analysis of denatured proteins: inclusion of denatured proteins in the reference set. Anal. Biochem. **214**, 17–24 (1993)

50. Griebenow, K., Klibanov, A.M.: On Protein Denaturation in Aqueous-Organic Mixtures but Not in Pure Organic Solvents. J. Am. Soc. Chem. **118**, 11695–11700 (1996)

51. Redfield, C., Dobson, C.M.: Sequential ^{1}H NMR assignments and secondary structure of hen egg white lysozyme in solution. Biochemistry **27**, 122–136 (1988)

52. Buck, M., Boyd, J., Redfield, C., MacKenzie, D.A., Jeenes, D.J., Archer, D.B., Dobson, C.M.: Structural determinants of protein dynamics: analysis of ^{15}N NMR relaxation measurements for main-chain and side-chain nuclei of hen egg white lysozyme. Biochemistry **34**, 4041–4055 (1995)

53. Strynadka, N.C.J., James, M.N.G.: Lysozyme revisited: crystallographic evidence for distortion of an N-acetylmuramic acid residue bound in site D. J. Mol. Biol. **220**, 401–424 (1991)

54. Cheetham, J.C., Artymiuk, P.J., Phillips, D.C.: Refinement of an enzyme complex with inhibitor bound at partial occupancyl hen egg-white lysozyme and tri-N-acetylchitotriose at 1.75 Å resolution. J. Mol. Biol. **224**, 613–628 (1992)

55. Hadfield, A.T., Harvey, D.J., Archer, D.B., MacKenzie, D.A., Jeenes, D.J., Radford, S.E., Lowe, G., Dobson, C.M., Johnson, L.N.: Crystal structure of the mutant D52S hen egg white lysozyme with an oligosaccharide product. J. Mol. Biol. **243**, 856–872 (1994)

56. Moorman, V.R., Valentine, K.G., Wand, A.J.: The dynamical response of hen egg white lysozyme to the binding of a carbohydrate ligand. Protein Sci. **21**, 1066–1073 (2012)

57. Blundell, C.D., DeAngelis, P.L., Day, A.J., Almond, A.: Use of ^{15}N-NMR to resolve molecular details in isotopically-enriched carbohydrates: sequence-specific observations in hyaluronan oligmers up to decasaccharides. Glycobiology **14**, 999–1009 (2004)

58. Bates, R.G., Pawlak, Z.: Solvent effects on acid-base behavior: five uncharged acids in water-sulfolane solvents. J Sol Chem **5**, 213–222 (1976)

59. DeMuth, J.C., McLuckey, S.A.: Electrospray droplet exposure to organic vapors: metal ion removal from proteins and protein complexes. Anal. Chem. **87**, 1210–1218 (2015)

60. Hopper, J.T.S., Sokratous, K., Oldham, N.J.: Charge state and adduct reduction in electrospray ionization-mass spectrometry using solvent vapor exposure. Anal. Biochem. **421**, 788–790 (2012)

61. Hunter, E.P., Lias, S.G.: Evaluated gas phase basicities and proton affinities of molecules: an update. J. Phys. Chem. Ref. Data **27**, 413–656 (1998)